



# A hybrid room acoustic approach for auralization

Wouter Wittebol<sup>1,a</sup>, Maarten Hornikx<sup>1,b</sup>

<sup>1</sup>Department of the Built Environment, Eindhoven University of Technology,  
P.O. Box 513, 5600 MB Eindhoven, The Netherlands

<sup>a</sup>w.wittebol@tue.nl, <sup>b</sup>m.c.j.hornikx@tue.nl

## Abstract

The challenge in creating computational models for room acoustical auralizations lies in maintaining perceptual credibility while keeping computational demand within bounds. Wave-based solvers can accurately describe all wave phenomena but do so at an increasing computational cost for increasing frequencies. In this work, a hybrid approach that combines the following parts is presented. Firstly, a time-domain wave-based method is used for the low frequency range where the mesh can be coarse, at a limited computational demand. Secondly, an image source model is combined with a diffusion equation model for the high frequency range. Here the image source model is used to calculate the early specular part of the impulse response, and the diffusion equation model is used to describe the late diffuse part of the impulse response. This paper elaborates on the details of this approach and its application to produce room impulse responses. A comparison between room impulse responses created with this approach and those created with a reference wave-based solver for a benchmark room is given.

**Keywords:** room acoustics, auralization, hybrid model, image source model

## 1 Introduction

Nowadays more and more aspects of a building can be experienced before its realisation with the help of virtual reality. Where traditionally in the design phase, a building was solely described using two-dimensional drawings, nowadays virtual reality makes it possible for project stake-holders to walk through a fully-fledged digital copy of a building. Though there has been a lot of advancement in the visual representation of buildings during the design phase, the acoustical representation somewhat lingers as it is still mainly conveyed in terms of room acoustical parameter values displayed on floor plans using coloured grids, or plainly as numerical values in tables. Auralization being the acoustical equivalent of visualization can provide an acoustic experience embedded in a 3D VR environment. Current limitations regarding the application of auralization for VR environments are mainly related to the trade-off between computational demand and accuracy. Providentially, for applications in the built environment, a state-of-the-art low latency real-time auralization engine is not essential, but it remains crucial that the acoustical performance of a room's design can be simulated and conveyed to stake-holders within a limited time frame while preserving accuracy.

Room acoustic prediction methods are based on numerical, statistical or geometrical descriptions of physical phenomena, with geometrical methods being most commonly used. Geometric acoustical methods are generally quick but assume sound to behave as rays, and diffraction effects are commonly not considered which for instance causes non-physical acoustical shadowing effects, and diffraction based scattering. Wave-based approaches can be used to solve all relevant wave-behaviour (reflection, diffraction and interference) with high accuracy, but the size and geometrical complexity of rooms commonly encountered in the built environment limits their application to the low-frequency range where a coarser mesh with a limited computational demand suffices. Statistical methods are generally fast, but assume a diffuse sound field and do not take the distinct

characteristics of early reflections into account. Hybrid room acoustical models that combine different room acoustical modelling techniques while playing in to their individual strengths and weaknesses can provide a solution.

In this research three different room acoustical modelling techniques with distinct strengths and weaknesses are combined into such a hybrid. Firstly, the time domain discontinuous Galerkin (DG) wave-based method is used to calculate the low frequency range. And secondly, a combination of the image source model (ISM) and an acoustic diffusion equation (DE) model is used to represent the respectively specular and non-specular contribution to the sound field for the high frequency range. In section 2, this hybrid model is introduced followed by a brief introduction on the three used modelling approaches. Section 4 presents the results and discussion of room impulse responses generated with the hybrid model compared to a fully wave-based simulation for two different acoustical lay-outs of a room. Lastly, conclusions will be given in section 5.

## 2 Method

Figure 1 shows an overview of the hybrid model, the part demarcated by the black dotted rectangle is designated to generating the non-specular part of the high frequency impulse response, the part demarcated by the red dotted rectangle is designated to generating the specular part of the high frequency impulse response which is solved by the ISM, and the part demarcated by the blue dotted rectangle is designated to generating the low-frequency impulse response which is solved using the DG method. In the black rectangle we generate build-up envelopes per octave band using an analytical formula which will be called non-specular envelope (NSE) formula from now on, and envelopes per octave band generated with the DE model. The build-up envelope, and the DE envelope are used for before and after the transition point  $t_c$  respectively. the build-up envelope is scaled to match the DE envelope at  $t_c$ , and these envelopes are concatenated. Then a two-term exponential fitting is applied to create an analytical non-specular envelope from these concatenated envelopes. Random noise (RN) is generated, and filtered by octave band pass filters (BPF), this random noise is shaped by the non-specular envelopes per band. These bands are then summed to create a broad-band non-specular impulse response. Subsequently this non-specular impulse response is added to the specular impulse response to create the impulse response for the high frequency part of the model. This high frequency impulse response is highpass filtered at the cross-over frequency  $f_c$ , and will be added to the wave-based impulse response which is low-passed at  $f_c$  to create the full hybrid impulse response. The different parts of the model depicted in this block diagram will be further elaborated on in section 2.1.

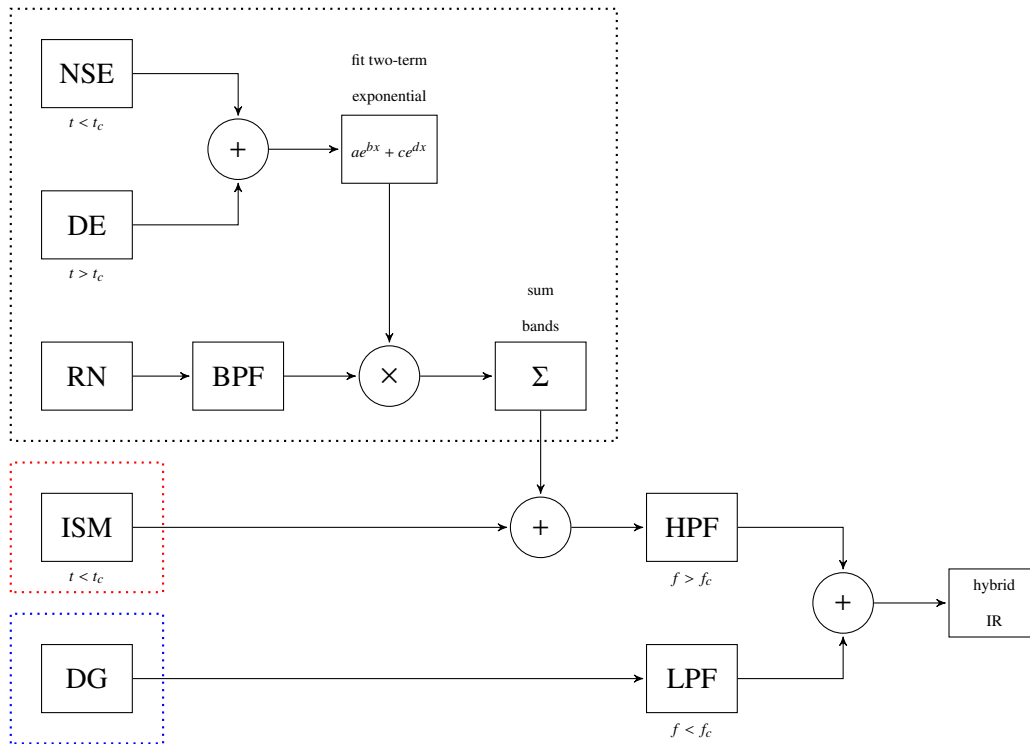


**Figure 1.** Block-diagram of DG / (ISM + DE) hybrid model

- ... high frequency part (non-specular)
- ... high frequency part (specular)
- ... low-frequency part
- NSE** non-specular envelope formula  $< t_c$  (per octave band)
- DE** diffusion equation model  $> t_c$  (per octave band)
- RN** random noise generator (uniform distribution)
- ISM** image source model ( $< t_c$ )
- DG** time domain discontinuous galerkin method
- BPF** band-pass filter
- LPF** low-pass filter
- HPF** high-pass filter
- $t_c$  transition time
- $f_c$  cross-over frequency

## 2.1. Hybrid model

With the ISM and the DE model we have a way to describe two extreme types of sound fields, namely a specular and a diffuse sound field. Since the sound field in a room transitions gradually from a specular (early reflections) to a diffuse sound-field (reverberation tail), we need a component to describe the non-specular contribution to the sound field during this transition. This transition process can be described using the analogy of a single sound wave that progressively relinquishes its specular energy to the non-specularly reflected sound field due to its successive interactions (orders) with boundary surfaces (see Figure 2) (4). If a room is compact in shape and with its materials homogeneously distributed, we can apply this analogy to help shaping a gradual transition from a specular to a diffuse sound field, since all occurring sequences of reflections can be assumed to behave in a similar manner, and we can assume two subsequent reflections to be separated by one mean free path length  $\bar{r}$ . We can then relate the reflection order  $n$  to time  $t$  via the relation with the speed of sound  $c$ ,

$$t = n \cdot \frac{\bar{r}}{c} \quad (1)$$

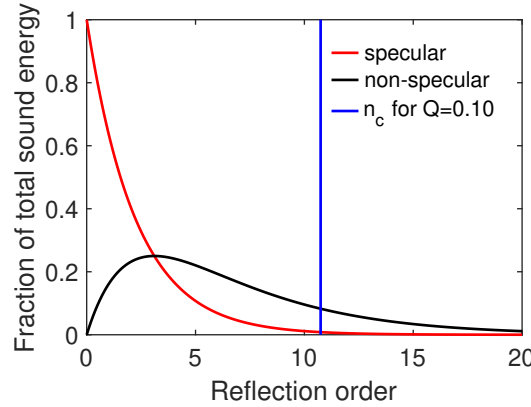


**Figure 2.** Conversion of specularly reflected sound energy to non-specularly reflected sound energy (when absorption coefficient  $\bar{\alpha} = 0.2$  and scattering coefficient  $\bar{s} = 0.2$ )

In this case the specularly ( $W_s$ ) and non-specularly ( $W_{ns}$ ) reflected fraction of the sound energy are described in terms of the reflection order  $n$  using the average scattering  $\bar{s}$  and average absorption  $\bar{\alpha}$  coefficients of the boundary surfaces as,

$$W_s(n) = ((1 - \bar{s}) \cdot (1 - \bar{\alpha}))^n, \quad (2)$$

$$W_{ns}(n) = (1 - (1 - \bar{s})^n) \cdot (1 - \bar{\alpha})^n, \quad (3)$$

where  $\bar{\alpha}$  and  $\bar{s}$  are determined as,

$$\bar{\alpha} = \frac{\sum_{i=1}^n A_i \cdot \alpha_i}{\sum_{i=1}^n A_i}, \quad (4)$$

$$\bar{s} = \frac{\sum_{i=1}^n A_i \cdot s_i}{\sum_{i=1}^n A_i}, \quad (5)$$

where  $A_i$  is the surface area of the material,  $\alpha_i$  is the random-incidence absorption coefficient of the material, and  $s_i$  is the random-incidence scattering coefficient of the material.

The ratio between the specular and non-specular sound field energy can be described as,

$$Q(n) = \frac{(1 - \bar{s})^n}{1 - (1 - \bar{s})^n}, \quad (6)$$

which is only dependent on  $\bar{s}$ . By solving equation (6) for  $n$  we obtain the reflection order at which a given specular to non-specular ratio  $Q$ ,

$$n(Q) = \frac{\ln\left(\frac{Q}{Q+1}\right)}{\ln(1 - \bar{s})}. \quad (7)$$

This order is shown as  $n_c$  in Fig. 2 for a  $Q$  of 0.10.

### Connecting the non-specular build-up envelope to the DE envelope

From the DE model we acquire an energy vs. time envelope per frequency band. The time  $t_c$  at which a low enough  $Q$ -value is reached, or in other words at which the sound field in the room is diffuse enough to be described by the DE model can be approximated from the order  $n$  and the mean free path length  $\bar{r}$  via equation (1). The non-specular contribution up until  $t_c$  is described using equation (3), since this equation only gives us an approximation of which part of the sound field is non-specularly reflecting at a given instance, we use the value of the DE envelope at  $t_c$ , and scale the value of the build-up envelope to match that value. Subsequently the beginning of the DE envelope and the end of the build-up envelope are truncated at  $t_c$ , after which they are concatenated together.

### Fitting a two-term exponential to the combined envelopes

To address a possible discontinuity at the point where the analytical envelope and DE envelope are connected (denoted with  $\times$  in Fig. 3), a continuous envelope is generated using a two-term exponential fitting,

$$y(x) = a_1 \cdot e^{a_2 \cdot x} + a_3 \cdot e^{a_4 \cdot x}, \quad (8)$$

with MATLAB's curve fitting toolbox. Note that in Fig. 3 we see the square root of the energy envelope, this is because it will later on be combined with the ISM which is a pressure-based model.

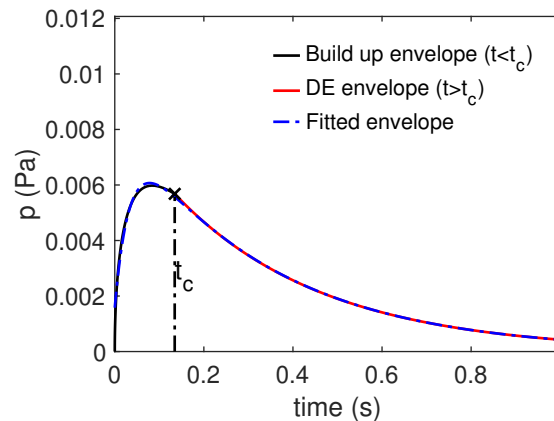


**Figure 3.** Fitting exponential function to combined build-up and DE envelopes example

From this fitting we acquire a fully analytical non-specular envelope (equation (3)), of which the coefficients ( $a_1, a_2, a_3, a_4$ ) are determined partly by the shape of the build-up envelope and partly by the shape of the DE envelope. Note that equation (3) can also be written as a two-term exponential of base  $e$  as,

$$W_{ns}(n) = e^{\ln(1-\bar{\alpha})n} - e^{\ln((1-\bar{\alpha})(1-\bar{s}))n}. \quad (9)$$

Then  $W_{ns}$  is described as a function of time using  $n = t \cdot c/\bar{r}$ , this results in,

$$W_{ns}(t) = e^{\ln(1-\bar{\alpha})(c/\bar{r})t} - e^{\ln((1-\bar{\alpha})(1-\bar{\delta}))(c/\bar{r})t}. \quad (10)$$

A set of initial values ( $a_{1i}, a_{2i}, a_{3i}, a_{4i}$ ) for the fitting algorithm are obtained from this description of the build-up envelope described by equation (10) as  $a_{1i} = Q_{ns}$ ,  $a_{2i} = \ln(1-\bar{\alpha})(c/\bar{r})$ ,  $a_{3i} = -Q_{ns}$ , and  $a_{4i} = \ln((1-\bar{\alpha})(1-\bar{\delta}))(c/\bar{r})$ . Note that  $Q_{ns}$  is the scaling factor to make the amplitude of the analytical envelope match that of the DE envelope at  $t_c$ .

### Non-specular part of sound field as a random process

A sound field is diffuse when all directions of sound propagation have equal probability of occurring and consequently contribute equal sound energy (4). This type of sound field can be represented using a random process with a uniform probability density function (6) (see equation 11). For a uniformly distributed noise signal the probability density function is

$$f(x) = \begin{cases} \frac{1}{b-a} & \text{for } a \leq x \leq b, \\ 0 & \text{for } x < a \text{ or } x > b. \end{cases} \quad (11)$$

We want a noise signal on the range  $[-1, 1]$  so we take  $a = -1$  and  $b = 1$ . This signal has a standard deviation  $\sigma = \sqrt{1/3}$ , and a mean  $\mu = 0$ .

### Band filtering

In the non-specular high frequency part of the model Butterworth filters are used to band-pass filter white noise into octave bands. A Butterworth filter is also used to low-pass filter the low-frequency part of the hybrid impulse response and to high pass filter the high-frequency part of the hybrid impulse response. The magnitude of these filters at their cut-off frequencies should lie at  $1/2$  which is the case for a pass-band gain adjustment factor ( $\epsilon$ ) of 1,

$$\epsilon = \sqrt{10^{-0.1 \cdot a_{pass}} - 1}. \quad (12)$$

The Butterworth filter's magnitude response (low-pass) (8) is described by,

$$|H| = \frac{1}{\sqrt{1 + \epsilon^2 \cdot (\omega/\omega_0)^{2n}}}. \quad (13)$$

The Butterworth filter is described in terms of its pass-band attenuation ( $a_{pass}$ ), pass-band frequency ( $\omega_{pass}$ ), its stop-band attenuation ( $a_{stop}$ ), and stop-band frequency ( $\omega_{stop}$ ). From these design parameters the minimum filter order is determined using

$$n_{filter} = \frac{\log_{10} \left( \frac{10^{-a_{pass}/10} - 1}{10^{-a_{stop}/10} - 1} \right)}{2 \cdot \log_{10} \left( \frac{\omega_{pass}}{\omega_{stop}} \right)}. \quad (14)$$

For the Butterworth filters a pass-band attenuation of 3.02 dB was used and a stopband attenuation of 80 dB. This minimum filter order together with the desired passband frequencies ( $\omega_{passL}, \omega_{passH}$ ) are used as the input to MATLAB's **designfilt** function to establish infinite impulse response Butterworth band-passfilter's. These filters are used to filter the random noise in the non-specular part of the hybrid.

Infinite impulse response filters have non-linear phase but since we are able to filter off-line MATLAB's zero phase **filtfilt** function could be used. Note that while applying the filter it is necessary to padd the signal with a sufficient amount of zeros  $\nu$  (2),

$$\nu = \lceil (3/2) \cdot n_{filter} \cdot fs / f_{Lmin} \rceil. \quad (15)$$

It is evident from this formula that the amount of zeros needed for the padding increase with filter order  $n_{filter}$ , and with an increasing sampling frequency to pass-band frequency ratio, hence the lowest frequency band's lower frequency limit ( $f_{Lmin}$ ) is normative when it comes to determining the padding. Half of the required zeros are padded in front of the signal and half after the signal.

## 2.2. Wave-based solver Time-domain Discontinuous Galerkin Method (TD-DG)

TD-DG is a time domain wave-based simulation method which solves linear acoustic equations by discretizing the simulation domain into finite elements. It uses an unstructured mesh which allows for local refinements making it possible to accurately simulate complex geometries without having to approximate shapes. The method solves the governing equations element-wise which makes it computationally expensive for serial processing, but this element-wise computation lends itself well to parallel processing (9). The TD-DG model works with locally reacting impedance boundary conditions. These boundary conditions can use the impedance-values calculated with the impedance models described in section 3. The simulated source is a Gaussian pulse as described in Ref. (10). The spectral characteristics of this pulse are also present in the simulated impulse responses. To remove these characteristics an analytical inverse filter was used.

## 2.3. Image source model

The image source method is a deterministic algorithm that can be applied to construct a room impulse response from all possible specular reflection paths between transducer positions (source position(s) and receiver position(s)) in a room. The image source method can be applied in the time domain (1) but also in the frequency domain (5). The advantage of a frequency domain application over a time domain application is that in a frequency domain application the phase delays are not limited to integer multiples of the sampling period (5). The model developed in this study is a frequency domain model that works for rooms that are geometrically speaking a convex polyhedron, where it is made possible to define polygons with different boundary conditions on its bounding surfaces.

We will commence from the point where a set of valid image sources is defined. The contribution of an image source  $k$  to the total sound field can be described using a set of phasors  $X_k$ , which is defined as

$$X_k(\omega) = A_k(\omega) \cdot e^{i\phi_k(\omega)}. \quad (16)$$

$X_k$  consists of an attenuation factor  $A_k$  and a frequency dependent shift in phase  $e^{i\phi_k}$ .  $A_k$  depends on the directivity factors at the source  $Q_{s_k}$  and at the receiver  $Q_{r_k}$  for their given angles of incidence (which are angle-independent in the case of omni-directional transducers), the total reflection coefficient  $R_{tot_k}$ , the part relinquished to the non-specular field due to scattering  $S_{tot_k}$ , and the attenuation due to the total reflection path length  $r_k$  or similarly the distance between an image source and the receiver.

$$A_k(\omega) = \frac{Q_{s_k} \cdot Q_{r_k} \cdot R_{tot_k} \cdot S_{tot_k}}{4\pi \cdot r_k} \quad (17)$$

The reflection coefficient for an interaction with a bounding surface depends on the frequency dependent specific impedance of the material of that surface  $\zeta$  and the angle of incidence to the normal of that surface  $\theta$ .

$$R = \frac{\zeta \cdot \cos \theta - 1}{\zeta \cdot \cos \theta + 1} \quad (18)$$

The total reflection coefficient of an image source contribution can then be calculated as

$$R_{tot_k} = \prod_{i=1}^n R_i, \quad (19)$$

where  $n$  is the number of wall interactions for a given image source.  $R_i$  is the  $i$ -th encountered wall reflection coefficient.

The frequency dependent scattering coefficient  $s$  is defined as the part of the sound that is reflected in a non-specular direction upon wall interaction, this results in a reduction of the specular field of  $S$ .

$$S = (1 - s) \quad (20)$$

The total reduction due to scattering of an image source contribution can then be calculated as

$$S_{tot_k} = \prod_{i=1}^n S_i. \quad (21)$$

With the time delay  $t_{0_k}$  corresponding to the image source receiver distance  $r_k$  for a given image source  $k$  ( $t_{0_k} = \frac{r_k}{c}$ ), the corresponding phase  $\phi$  for a given frequency  $l$  can be calculated as follows,

$$\phi_k(\omega) = \omega \cdot t_{0_k}. \quad (22)$$

The room's transfer function  $H(\omega)$  is constructed by summing all the image source contributions per frequency,

$$H(\omega) = \sum_{k=1}^N X_k(\omega). \quad (23)$$

Subsequently the room's impulse response can be obtained by applying an inverse Fourier transform to the room's transfer function,

$$h(t) = \mathcal{F}^{-1}\{H(\omega)\}. \quad (24)$$

#### 2.4. Acoustic diffusion equation model

The acoustic DE model describes sound propagation as a diffusion process. It is strongly dependent on the so-called diffusion coefficient which determines the rate at which sound diffuses within a room. This diffusion coefficient is a function of the speed of sound, and the mean free path length. The DE model holds for nearly-isotropic fields only, i.e. a highly diffuse sound field (4). It was originally proposed by Ollendorf (7) as a method to predict the diffuse sound field in rooms because it is more general than Sabine theory in a sense that it allows for local variations of the energy density.

### 3 The benchmark cases

#### 3.1. Room layout

Two scenarios mimicking common acoustical conditions of office spaces were created by retrofitting a reverberation chamber with acoustical panels, carpet tiles, and office furniture. The empty room has an internal volume of 89 m<sup>3</sup> and a ceiling height of 3.3 m. For the first scenario the room underwent a more substantial acoustical treatment than for the second scenario. The first scenario is also equipped with more office furnishing. Figures 4a and 4b show the geometrical models of scenario I and II respectively that were used to generate the mesh with Gmsh for the DG wave-based solver. Since the ISM was designed only for simulating convex rooms with polygons on the bounding surfaces, the models used for the high frequency part (ISM and DE) of the hybrid were simplified by excluding the furniture, the recessions in the wall (East), the door (South), and the window rebates (East) from the model, see Figs. 4c and 4d.

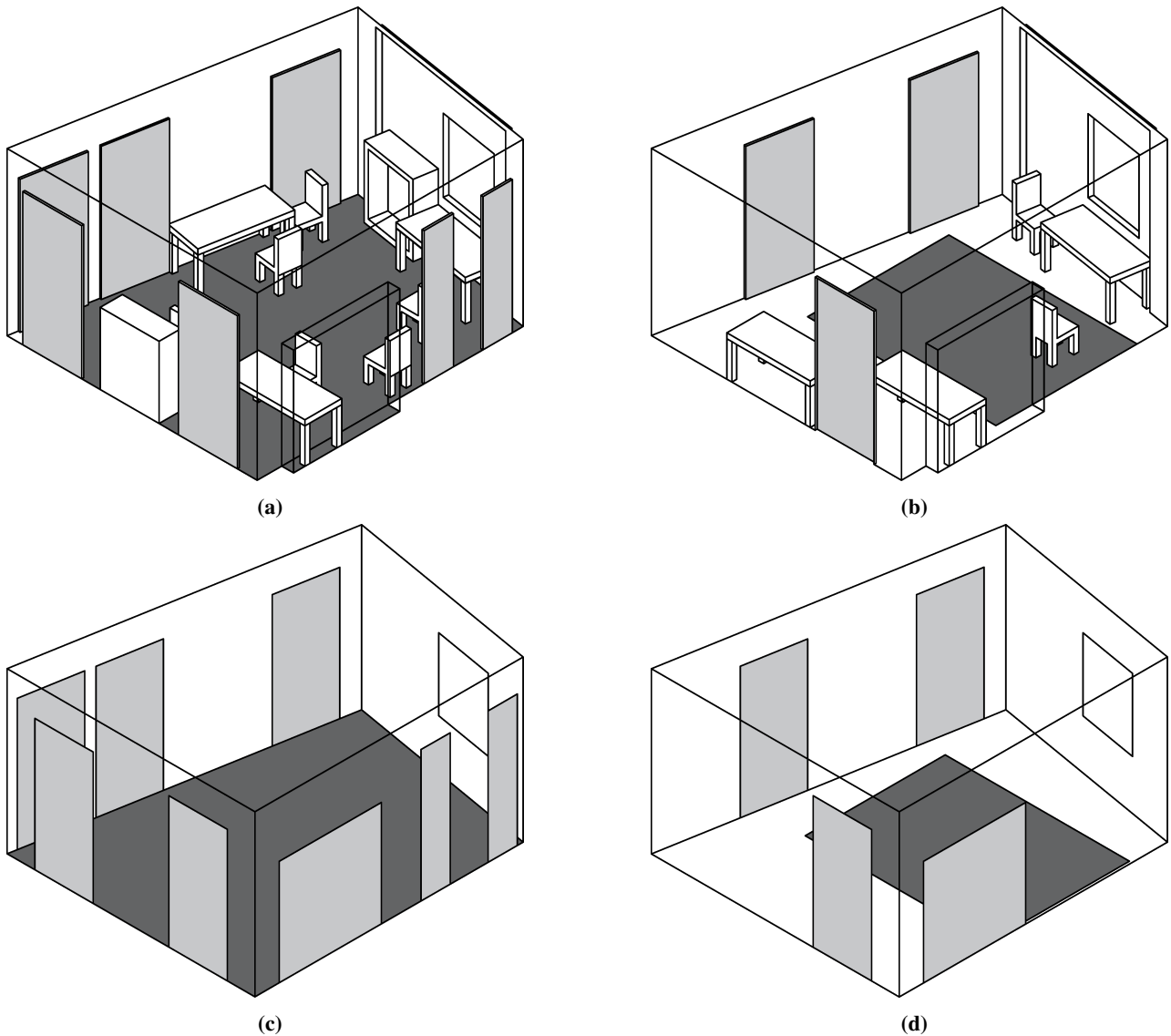
#### 3.2. Transducer positioning

Figure 5 shows the source and receiver positions used for the simulation. The source is located at [ $x = 3.01$  m,  $y = 2.64$  m,  $z = 1.62$  m] and the receiver is located at [ $x = 4.26$  m,  $y = 1.76$  m,  $z = 1.62$  m] with the origin at the  $\times$  in the left bottom corner of the room. The transducer positioning was kept equal for both scenarios.

#### 3.3. Boundary conditions

##### Boundary conditions for the ISM and the TD-DG model

Impedance models were used to characterise the acoustical treatments in the room (panels and carpets), parameter values for these models were taken from a reference study (3). For the ISM these impedance



**Figure 4.** 3D models for: (a) Scenario I DG, (b) Scenario II DG, (c) Scenario I ISM & DE, (d) Scenario II ISM & DE

models could be used as such, while for the TD-DG model these impedance values were cast into time domain boundary conditions (9). The reflective characteristics of the walls, door, and window were modelled as frequency independent and real-valued ( $R = 0.996$ ).

#### **Boundary conditions for the diffusion equation model**

The DE model does not work with complex-valued angle dependent reflection coefficients but uses the real-valued random incidence absorption coefficient. The random incidence absorption  $\alpha_{uni}$  is calculated from the complex valued impedances using the Paris formula (4). Furthermore the ISM has a fine frequency resolution (e.g.  $\Delta f = 0.5\text{Hz}$ ), while the DE model needs to run separate instances of the simulation for each set of absorption coefficients  $\alpha_{uni}$  assigned to the materials for a given frequency, hence using a high frequency resolution is not practical, so instead an octave band resolution is used. Figure 6 shows the random incidence absorption coefficients, and the octave resolution averaged random incidence absorption coefficients  $\bar{\alpha}_{uni}$  for the panel (Fig. 6a) and the carpet (Fig. 6b).

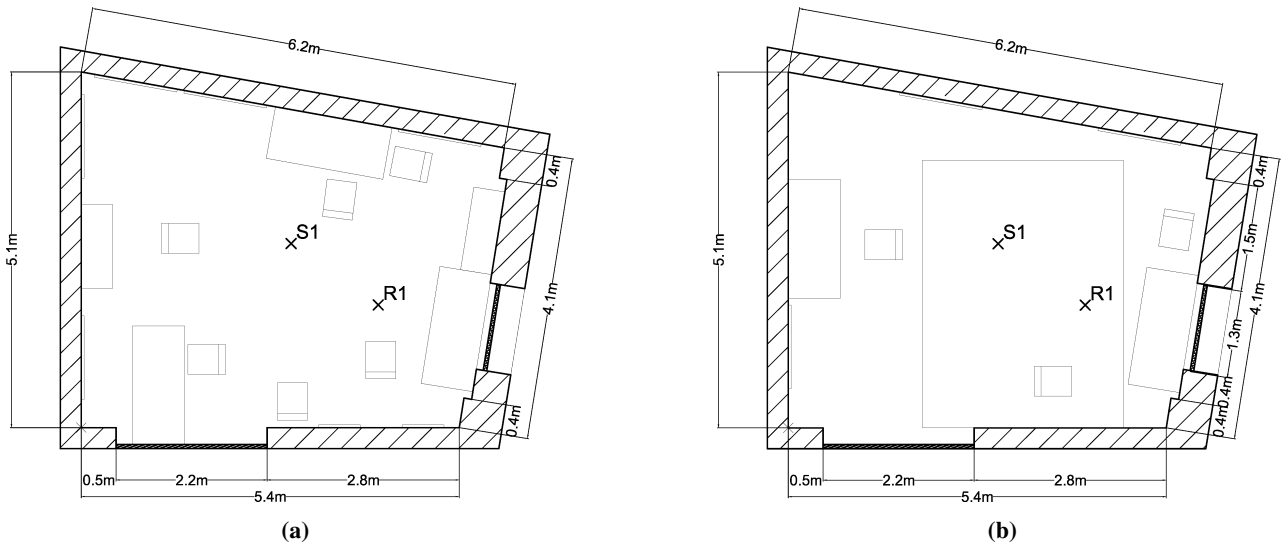


Figure 5. Source and receiver positions for scenario I (a) and scenario II (b)

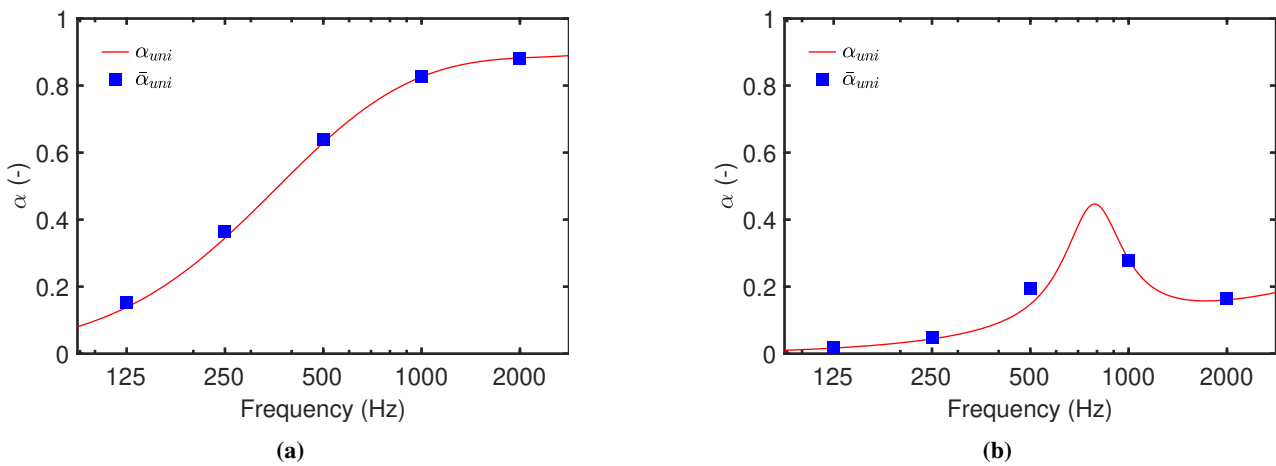


Figure 6.  $\alpha_{umi}$ , and  $\bar{\alpha}_{umi}$  values for acoustic panels (6a) and carpet (6b)

### Scattering coefficients

Since the scattering coefficient is used to describe the effects of scattering due to diffraction effects as well as surface roughness it proved difficult to come up with well substantiated method for determining these scattering coefficients. The used scattering coefficients are shown in Table 1, the same scattering coefficients were applied to all materials in the ISM. Scenario I was given higher scattering coefficients than scenario II since it has significantly more furniture, and also more acoustical treatments.

Table 1. Averaged scattering coefficients ( $\bar{s}$ ) for scenario I and scenario II

Frequency (Hz)	125	250	500	1000	2000
$\bar{s}$ (scenario I)	0.15	0.25	0.50	0.53	0.55
$\bar{s}$ (scenario II)	0.12	0.15	0.25	0.33	0.35

## 4 Results and discussion

Table 2 and 3 show a comparison of the reverberation times  $T_{20}$ -values obtained for the benchmark cases (scenario I and II) using the reference wave-based solver (DG), the separate DE model, the hybrid model (ISM+DE) and the full hybrid model (ISM+DE+DG). The  $T_{20}$ -values were obtained using the integrated impulse response method as described in the ISO 3382 standard.

**Table 2.**  $T_{20}$  comparison DG, DE, IS+DE, and full hybrid (FH) scenario I

Frequency (Hz)	125	250	500	1000	2000
$T_{20}$ (s) DG	3.4	1.2	0.6	0.6	0.6
$T_{20}$ (s) DE	2.8	1.2	0.6	0.5	0.5
$T_{20}$ (s) IS+DE	3.1	1.3	0.7	0.4	0.5
$T_{20}$ (s) FH	3.4	1.3	0.7	0.4	0.5

**Table 3.**  $T_{20}$  comparison DG, DE, IS+DE, and full hybrid (FH) scenario II

Frequency (Hz)	125	250	500	1000	2000
$T_{20}$ (s) DG	4.2	2.3	1.1	0.9	0.9
$T_{20}$ (s) DE	3.8	2.4	1.2	0.9	0.9
$T_{20}$ (s) IS+DE	4.2	2.3	1.2	0.8	0.9
$T_{20}$ (s) FH	4.2	2.3	1.2	0.8	0.9

The low-frequency agreement in the  $T_{20}$ -values between DG and the ISM+DE-part of the model is better than the agreement between DG and the DE-part of the model for both scenarios. This improvement can be attributed to the fact that the ISM part of the hybrid model incorporates the distinct specular reflections and interference effects in the early part of the impulse response, while the DE model alone merely provides a decay envelope for a diffuse sound field.

The IS+DE model still shows a deviation from the DG model in the 125 Hz band for scenario I. This is possibly due to diffraction effects, these effects are not modelled in the ISM+DE part of the model and scenario I has a significant amount of furnishing that causes diffraction effects in the lower frequency range. This means that it would be beneficial to model diffraction for that frequency range in this case. This problem is addressed in the full hybrid (FH) since here the lower frequency range  $< f_c$  is simulated with the wave-based solver and so diffraction is incorporated. Lower average scattering coefficients  $\bar{s}$  at a given frequency band make that the ISM part of the impulse response becomes more dominant while higher average scattering coefficients mean that the DE + non-specular part of the impulse response becomes more dominant.

Scattering is a result of diffraction or reflection. In addition, scattering also happens at different scale levels, i.e. the interior of the room (which is not modelled with the ISM+DE method) causes scattering at a larger scale, while the surface textures cause scattering at a smaller scale. So the effect of scattering at both scales is to be accommodated in the averaged scattering coefficient  $\bar{s}$ . The difficulty lies in finding appropriate scattering coefficients for a given room acoustical scenario.

Furthermore the build-up envelope describing the non-specular part of the sound field ( $< t_c$ ) depends on the averaged absorption and scattering coefficients.  $t_c$  from which onwards the DE model is used to describe the non-specular contribution to the sound field depends on averaged scattering coefficients. The use of these

averaged coefficient strictly only makes sense when all specular sounds paths in the room have a comparable sequence of interactions with their bounding surfaces, in terms of the amount of interactions per time frame and in terms of the scattering and absorption properties they encounter with each interaction. This means that for instance the room shouldn't be very elongated since then the reflection density of sound paths in the long direction will deviate significantly from the reflection density of sound paths in the short direction. Also the material distribution should be relatively homogeneous.

## 5 Conclusions

A hybrid room acoustical approach combining the image source method + DE method (high frequency range) with the time-domain discontinuous Galerkin method (low-frequency range), this hybrid was compared to a reference wave-based solver in terms of reverberation time for two benchmark cases. The benchmark cases were simulated using solely the DE model, a hybrid of the DE model + ISM model, and the full hybrid model (ISM+DE+DG) respectively. It showed that the agreement between the reference wave-based solver improved with increasing hybrid complexity. The most challenging aspects regarding the further development of this model will lie in the correct determination of the transition time  $t_c$  for the high frequency part of the model (scattering coefficients), and in the determination of the cross-over frequency  $f_c$  between the low frequency (TD-DG) part of the model and the high frequency part (ISM+DE).

## Acknowledgements

This work was supported by funding from Facebook Technologies, LLC.

## References

- [1] ALLEN, J. B., AND BERKLEY, D. A. Image Method for Efficiently Simulating Small-room Acoustics. *The Journal of the Acoustical Society of America* (1979), 943–950.
- [2] BOORE, D. M. On Pads and Filters: Processing Strong-Motion Data. *Bulletin of the Seismological Society of America* 95, 2 (2005), 745–750.
- [3] BRIERE DE LA HOSSERAYE, B., GEORGIU, F., HORNIKX, M. C. J., AND WANG, H. Derivation of time-domain surface impedance boundary conditions based on in-situ surface measurements and model fitting. In *Proceedings of the 23rd International Congress on Acoustics* (Aachen, Germany, Sept. 2019).
- [4] KUTTRUFF, H. *Room Acoustics*, 5th ed. CRC Press, 2009.
- [5] LEHMANN, E. A., AND JOHANSSON, A. M. Prediction of energy decay in room impulse responses simulated with an image-source model. *The Journal of the Acoustical Society of America* 124, 1 (2008), 269–277.
- [6] MEESAWAT, K., AND HAMMERSHØI, D. An investigation on the transition from early reflections to a reverberation tail in a brir. In *Proc. of the 2002 International Conference on Auditory Display* (Kyoto, Japan, July 2002).
- [7] OLLENDORF, F. Statistical Room-Acoustics as a Problem of Diffusion (A Proposal). *Acta Acustica united with Acustica* 21, 4 (1969).
- [8] THEDE, L. *Practical Analog and Digital Filter Design*, 1st ed. Artech House, 2004.
- [9] WANG, H., AND HORNIKX, M. Time-domain impedance boundary condition modeling with the discontinuous Galerkin method for room acoustics simulations. *The Journal of the Acoustical Society of America* 147, 4 (2020), 2534–2546.
- [10] WANG, H., SIHAR, I., PAGÁN MUÑOZ, R., AND HORNIKX, M. Room acoustics modelling in the time-domain with the nodal discontinuous Galerkin method. *The Journal of the Acoustical Society of America* 145, 4 (2019), 2650–2663.